CETRA2026 27-30 May 2026, Bol, Island Brač, Croatia
9th International Conference on Road and Rail Infrastructure

OPTIMIZATION OF A HYDROGEN-ENABLED MICROGRID FOR SEASONAL ENERGY STORAGE IN SUSTAINABLE RAILWAY INFRASTRUCTURE

Christoph Steindl[1], **Gerhard Fritscher**[1], **Julian Heger**[2]
[1]*University of Applied Sciences Technikum Wien, Austria*
[2]*ÖBB-Infrastruktur AG, Austria*

Abstract

The growing demand for reliable, sustainable energy supply solutions for railway infrastructure along secondary lines in remote areas calls for systems that can operate independently of the public grid. Combining renewable energy sources with seasonal energy storage, such as hydrogen, offers a promising solution for a sustainable, self-sufficient energy supply. In this context, the design of the energy system and the energy management strategy play a key role in achieving self-sufficiency, as well as a high level of reliability and efficiency. This study numerically investigates a hydrogen-enabled microgrid for powering an electric switch-point heating system at a railway site in Lower Austria, characterized by moderately cold climate conditions. The objectives of the study are to identify an optimized microgrid configuration and develop an optimized energy management strategy to ensure reliable, efficient operation and maximize renewable energy utilization. The results demonstrate the feasibility of using hydrogen as a seasonal energy storage medium to address the challenges posed by fluctuating renewable energy supply and high energy demand during winter months. Furthermore, the optimized hydrogen-enabled microgrid design and energy management strategy enable a seasonal balance between energy supply and demand, ensuring reliable and efficient operation while minimizing reliance on external, fossil-based energy sources.

Keywords: hydrogen, microgrid, seasonal energy storage, sustainable railway infrastructure, optimization

1 Introduction

Reliable winter operation of railway infrastructure relies on switch-point heating systems that prevent ice and snow from accumulating on switch-points [1]. For secondary lines and rural stations not connected to the traction power grid, sustaining this high-power seasonal load via the public grid can be expensive, challenging from a sustainability perspective, or simply infeasible [2]. Hydrogen-enabled microgrids offer a sustainable solution for energy independence and long-term energy storage, especially in challenging environments with seasonal mismatches between renewable energy supply and heating demand in winter [3, 4]. While hydrogen (H_2) technologies in rail applications have advanced in rolling stock and refueling infrastructure, stationary microgrids for powering auxiliary railway infrastructure have not yet been extensively researched [5, 6]. Furthermore, recent research on hydrogen-enabled microgrid sizing offers foundational methods but lacks focus on railway auxiliary loads [7, 8]. This study addresses these gaps through simulation-based optimization of the energy supply concept and energy management strategy for a hydrogen-enabled microgrid powering a switch-point heating system at a rural railway site in Lower Austria, with moderately cold winters.

The hydrogen-enabled microgrid combines a PV system (PVS), a H_2 energy storage system (HESS), and a battery energy storage system (BESS) to optimize reliability, efficiency, and renewable energy source use, aiming to maximize renewable energy utilization while ensuring consistent service during winter heating demand.

2 Methodology

This section gives an overview of the studied use case and the hydrogen-enabled microgrid setup. It also outlines the numerical methods used in the investigations.

2.1 Use case

This study investigates Gars-Thunau station on the Kamptal railway line in Lower Austria, a rural site exposed to winter frost and snow. For safe, reliable winter operations, the two switch-points at the site are heated by electric rods, with a maximum power demand of 13.8 kW. Data from the 2023/2024 heating season are presented in figure 1. Note that the time-series starts on July 1. It shows that the system is operated for about 144 hours, resulting in an energy demand of 2 MWh.

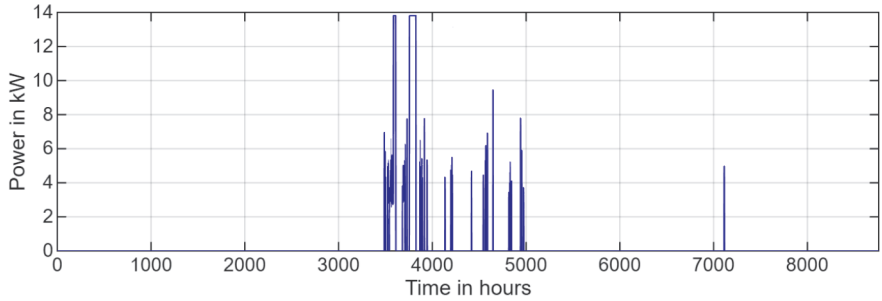

Figure 1 Switch-point heating system power demand for the 2023/2024 season

2.2 Microgrid system setup

The station under investigation is on a non-electrified line. In this context, an energy supply concept was developed in a previous concept study [3]. The concept highlighted in figure 2 includes a PVS, a short-term BESS, a seasonal HESS, a switch-point heating system, auxiliary loads, and an energy management system (EMS). Specifically, the HESS consists of an electrolyzer system (ELS) that converts excess summer electricity into H_2, a H_2 storage system (HSS), and a fuel cell system (FCS) that converts H_2 to electricity in winter. For more details, see the concept study [3]. Based on the results of the concept study [3], a first draft of the system is proposed, and selected components with their key parameters are listed in table 1.

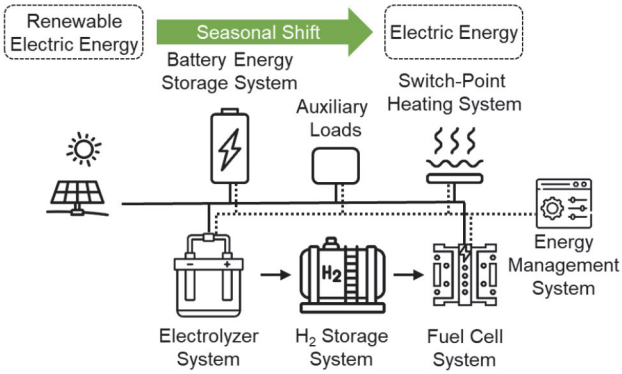

Figure 2 Setup of the hydrogen-enabled Microgrid adapted from [3]

Table 1 Input data of the hydrogen-enabled microgrid components

Subsystem	Component	Parameter and value
Renewable electric energy source	PV system	$P_{PVS,\,max} = 9.9\ kW_p$
HESS	Electrolyzer system	$P_{ELS,\,Module,\,nom} = 2,4\ kW_{el}$ ($n_{ELS,\,Module} = 2$)
HESS	H_2 storage system (metal hydride containers)	$M_{HSS,\,net} = 152\ kg$ ($m_{HSS,\,nom} = 160\ kg$)
HESS	Fuel cell system	$P_{FCS,\,Module,\,nom} = 4\ kW_{el}$ ($n_{FCS,\,module} = 4$)
BESS	Battery	$E_{BT,\,net} = 54\ kWh_{el}$ ($E_{BT,\,nom} = 60\ kWh_{el}$)
Auxiliary loads (permanent)	Safety-relevant components	$P_{Aux,\,perm} = 0.1\ kW_{el}$
Auxiliary loads (on-demand)	HSS balance-of-plant, H_2O treatment & H_2 purification components	$P_{Aux,\,od} = 0.366\ kW_{el}$

2.3 Modeling

The model of a hydrogen-enabled microgrid is set up in the MATLAB/Simulink simulation environment. The modeling focuses on the energy balance and energy management. Thus, a balance-based modeling approach, grounded in the concepts of Marocco et al. [9], is chosen to simulate the electrical energy and H_2 mass flows in the microgrid.

2.3.1 Photovoltaic system (PVS)

The PV generation profiles at hourly resolution are calculated using the PV*Sol premium 2025 [10] simulation software, based on regional climate data for a typical meteorological year (TMY) and technical data presented in [3] and in table 1.

2.3.2 Switch-point heating system

The switch-point heating system is modelled using the measured hourly load-demand profile presented in figure 1. Here, on/off switching dynamics are simulated to capture temporal patterns and operational constraints.

2.3.3 Auxiliary loads

The auxiliary load models are set up based on the technical parameters listed in table 1. Specifically, the modeled auxiliary loads are classified as either permanently operated or operated on demand when the corresponding processes are running.

2.3.4 Hydrogen energy storage system (HESS)

The HESS model comprises the FCS with proton-electrolyte-membrane (PEM) fuel cell stacks, the ELS with anion-exchange-membrane (AEM) electrolyzer stacks, and the HSS based on metal hydride technology submodels. The FCS and ELS are modelled based on literature polarization curves [11, 12], with the ELS/FCS stack power setpoint $P_{ELS/FCS,\ Stack}$ mapped to the ELS/FCS stack current $I_{ELS/FCS}$ according to equations (1), (2) and (3). Cell, stack and system specific data are assumed including, electrochemically active area (64 cm² for each electrolyzer cell and 100 cm² for each fuel cell), cell count of the electrolyzer/fuel cell stack $n_{FCS/ELS,\ Cell}$ (23 for the electrolyzer cell stack and 137 for the fuel cell stack) and module count of the electrolyzer/fuel cell modules $n_{FCS/ELS,\ Module}$ (table 1). Equations (2) and (3) consider the Balance of Plant (BOP) power consumption, assuming the BOP power share factor λ_{BOP} (0.097 for the ELS and 0.168 for the FCS) and the ELS nominal power $P_{ELS,\ Module,\ nom}$ (table 1).

$$P_{ELS/FCS,\ Stack} = n_{FCS/ELS,\ Cell} \cdot V_{ELS/FCS,\ Cell}(I_{ELS/FCS}) \cdot I_{ELS/FCS} \tag{1}$$

$$P_{ELS} = n_{ELS,Module} \cdot (P_{ELS,Stack} + P_{BOP}), \text{ with } P_{BOP} = \frac{\lambda_{BOP}}{1+\lambda_{BOP}} \cdot P_{ELS,Module,nom} \tag{2}$$

$$P_{FCS} = n_{Module,FCS} \cdot (P_{FCS,Stack} - P_{BOP}), \text{ with } P_{BOP} = \frac{\lambda_{BOP}}{1-\lambda_{BOP}} \cdot P_{FCS,Module} \tag{3}$$

Subsequently, the FCS hydrogen consumption rate $\dot{m}_{FCS,\ H2}$ and ELS hydrogen production rate $\dot{m}_{ELS,\ H2}$ are calculated based on previously determined ELS/FCS stack current $I_{ELS/FCS}$ using equation (4):

$$\dot{m}_{ELS/FCS,H_2}(t) = \frac{I_{ELS/FCS} \cdot M_{H_2}}{v \cdot F} n_{FCS/ELS,Cell} \cdot n_{ELS/FCS,Module} \tag{4}$$

Where M_{H2} corresponds to the molar mass of H_2 (2.02 g/mol), v represents the number of transferred electrons per hydrogen molecule (2) and F is the Faraday constant (96.485 C/mol). Furthermore, the HSS is modeled using the H_2 mass balance. Therefore, the Level of Hydrogen (LOH) is introduced and expressed by equation (5):

$$LOH(t+\Delta t) = LOH(t) + \frac{\dot{m}_{ELS,H_2}(t) \cdot \Delta t}{m_{HSS,nom}} - \frac{\dot{m}_{FCS,H_2}(t) \cdot \Delta t}{m_{HSS,nom}} \tag{5}$$

where $m_{HSS,\ nom}$ corresponds to the nominal capacity of the H_2 storage system, and Δt is the simulation time step (which is set to 1 hour in the present study).

2.3.5 Battery energy storage system (BESS)

The BESS is modeled using its State of Charge (SOC), which includes a calendar self-discharge rate r of 0.0028% per hour, corresponding to 2% per month. SOC dynamics are expressed with equation (6):

$$SOC(t+\Delta t) = SOC(t)\cdot(1-r\cdot\Delta t) + \frac{P_{BT,C}(t)\cdot\Delta t\Delta\eta_{BT,C}}{E_{BT,nom}} + \frac{P_{BT,D}(t)\cdot\Delta t}{\eta_{BT,D}\cdot E_{BT,nom}} \quad (6)$$

where $E_{BT,\,nom}$ represents the nominal energy capacity of the battery, $P_{BT,\,C/D}$ reflects the battery charging/discharging power (note that discharging power is per definition negative), and $\eta_{BT,C/D}$ is the battery charging/discharging efficiency, considering an average round trip efficiency of 95.7% [13].

2.3.6 Power electronics

The study uses average conversion efficiency data from commercially available power electronics within a similar power range [13]. Assuming an efficiency of 98.6% for the inverter and 98% for the DC/DC converters of PVS, FCS, ELS, and BESS.

2.3.7 Energy management strategy (EMS)

In this study, two EMSs were developed. These EMSs are based on rules for allocating power among the power generators, storage systems, and consumers. Decisions on power distribution rely on criteria based on inputs like consumers' demand, the PV system's current power output, the BESS's SOC, and the HSS's LOH. Both strategies prioritize PVS power to meet consumer demand. Surplus energy charges the BESS, then produces H_2 via ELS to fill the HSS. The difference between the two EMSs lies in the use of BESS. The "Aux-Battery" EMS uses the BESS to meet auxiliary power demand and converts hydrogen from HSS into electricity via FCS to meet switch-point heating system demand. The "Buffer-Battery" EMS discharges the BESS to meet short-term demand and converts H_2 to meet long-term demand. Both consider the physical and operational limits of BESS and HESS for safe and reliable operation.

3 Results and discussion

The initial evaluation using the simulation model is based on the first draft of the hydrogen-enabled microgrid concept presented in table 1 and the "Buffer-Battery" EMS. In figure 3, the LOH as well as the H_2 production and consumption rates are shown. A charge-sustaining operation regarding the LOH can be achieved throughout the entire 8, 760 hours. This means that when surplus electricity is available, H_2 is produced and stored, enabling sufficient availability in winter for conversion back into electricity using FCS to meet the electrical demand of the switch-point heating system. In summary, a grid-independent and reliable energy supply for the switch-point heating system can be ensured by using the HESS for seasonal storage and BESS for intra-day storage.

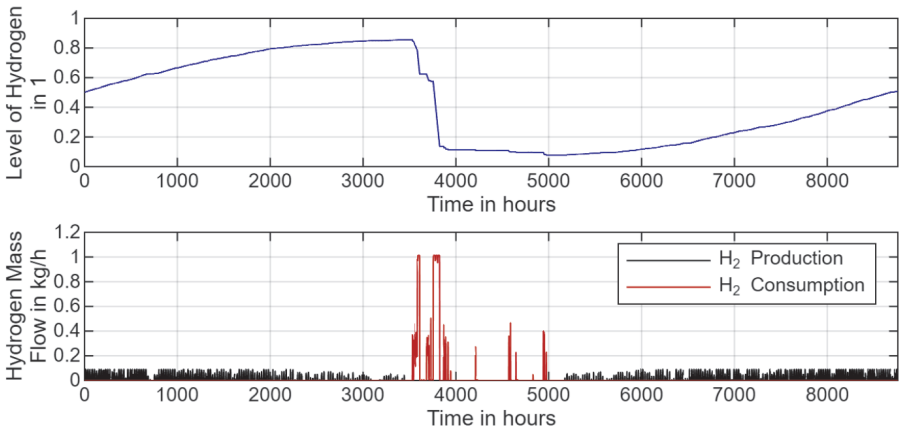

Figure 3 LOH and H_2 production and consumption rate over a year

3.1 Optimization of the EMS

As part of the EMS optimization, both EMS variants are evaluated using the microgrid's standard configuration (table 1). The results are presented in table 2. It is found that the "Buffer-Battery" EMS is superior to the "Aux-Battery" variant in terms of the hydrogen-enabled microgrid's overall efficiency. This is based on the fact that the HESS has a lower round-trip efficiency compared to the BESS. In detail, the "Aux-Battery" EMS leads to higher HESS utilization. However, because HESS has lower round-trip efficiency than BESS, the "Aux-Battery" EMS results in greater losses and lower overall efficiency compared to the "Buffer-Battery" EMS. Furthermore, the higher HESS utilization of the "Aux-Battery" EMS results in a negative H_2 balance under the given boundary conditions and assumptions. Consequently, charge-sustaining of the LOH cannot be achieved, which is necessary for grid-independent operation. As mentioned earlier, the "Buffer-Battery" EMS can ensure charge-sustaining operation regarding the LOH. Therefore, the "Buffer-Battery" EMS is preferred and will be used in further investigations.

Table 2 Results of EMS optimization

EMS variant	$m_{H_2, tot, cons}$ [kg]	$m_{H_2, tot, prod}$ [kg]	Difference [kg]
Aux-battery	130.9	127.7	-3.2
Buffer-battery	124.5	125.8	1.3

3.2 Sizing of energy storage components

To optimize the hydrogen-enabled microgrid's overall efficiency, sensitivity analyses are conducted on the ELS power, FCS power, and BESS capacity. Sensitivity analysis results for the electrolyzer system power indicate that increasing it reduces the total amount of H_2 produced, as shown in table 3. For the studied case, it can therefore be concluded that raising the ELS power leads to a significantly lower overall efficiency of the hydrogen-enabled microgrid. On the one hand, increasing the ELS power results in individual electrolysis modules operating at lower loads, thereby increasing efficiency. On the other hand, a greater ELS power also increases the power demand of the BOP components. Overall, it is found that raising the ELS power results in faster growth of BOP power demand than the efficiency gains achieved by operating the electrolyzer stacks at lower loads.

Consequently, this leads to less energy available for storage in the form of H_2 and finally, to reduced hydrogen-enabled microgrid's overall efficiency. Furthermore, note that with four ELS modules, insufficient LOH results in load shedding. This can be seen in table 3 from the reduced total H_2 mass consumed $m_{H2,\,tot,\,cons}$, compared to the variants with two and three ELS modules. Thus, an autonomous energy supply cannot be guaranteed at any time with the variant using four ELS modules.

Table 3 Sensitivity analysis results for electrolyzer system power

ELS Module Count	$P_{ELS,\,el,\,max,\,in}$ [kW_{el}]	$m_{H2,\,tot,\,cons}$[kg]	$m_{H2,\,tot,\,prod}$ [kg]	Difference [kg]
2	4.8	124.5	125.8	1.3
3	7.2	124.5	124.5	0.0
4	9.6	123.0	114.1	-8.9

Table 4 shows the results of the sensitivity analysis for the performance of the fuel cell system. Increasing the FCS power can improve the overall system efficiency. This is because, with increased FCS power, the individual FCS modules operate at lower loads and, consequently, at higher efficiencies. Finally, this results in lower hydrogen consumption while maintaining the same hydrogen production rate.

Table 4 Sensitivity analysis results for fuel cell system power

ELS Module Count	$P_{ELS,\,el,\,max,\,in}$ [kW_{el}]	$m_{H2,\,tot,\,cons}$[kg]	$m_{H2,\,tot,\,prod}$ [kg]	Difference [kg]
4	16	124.5	125.8	1.3
5	20	121.5	125.8	4.3
6	24	119.6	125.8	6.2

Another measure to enhance the overall efficiency of the hydrogen-enabled microgrid is to increase battery storage capacity, as shown by the sensitivity analysis results in table 5. Increasing the battery's storage capacity allows more energy to be stored and released. Consequently, less energy is stored as H_2 in the HESS and re-electrified via the FCS. Ultimately, this results in significantly lower H_2 consumption, while H_2 production decreases to a lesser extent.

Table 5 Sensitivity analysis results for battery energy storage capacity

$E_{BESS,\,nom}$ [kWh]	$m_{H2,\,tot,\,cons}$[kg]	$m_{H2,\,tot,\,prod}$ [kg]	Difference [kg]
60	124.5	125.8	1.3
80	123.3	125.5	2.2
100	122.3	125.2	2.9

4 Conclusion

This simulation study evaluated the concepts and energy management strategies of a hydrogen-enabled microgrid designed for a grid-independent, sustainable energy supply, using an electric switch-point heating system as an example. The results for the optimized energy management strategy indicate that employing a battery energy storage system as a buffer storage improves overall efficiency, whereas using it solely to power the auxiliary consumers is ineffective under the boundary conditions and assumptions.

Regarding the optimized system concept, increasing electrolyzer system capacity actually decreases overall efficiency, whereas raising the capacities of the fuel cell system and battery energy storage systems significantly enhances overall efficiency. In summary, the initial draft of the hydrogen-enabled microgrid configuration, combined with the "Buffer-Battery" energy management strategy, proves effective in achieving high overall efficiency while providing a grid-independent and sustainable solution for the energy supply of an electric switch-point heating system.

References

[1] Heger, J.: Inductive railway turnout heating systems – a review of scientific publications, 8th International Conference on Road and Rail Infrastructure - CETRA 2024, pp. 533-541, Cavtat, Croatia, 15-17 May 2024., https://doi.org/10.5592/CO/cetra.2024.1592

[2] Deng, H., Li, Y., Tang, C., Liu, J., Yi, Q., Wang, Y., Wang, P., Gao, M.: Green micro-grid for railway infrastructure, IEEE Transactions on Intelligent Transportation Systems, 26 (2025) 4, pp. 4346-4364, DOI: 10.1109/tits.2025.3544264

[3] Fritscher, G., Steindl, C., Helnwein, J., Heger, J.: Hydrogen-Enabled Microgrids for Railway Applications: A Seasonal Energy Storage Solution for Switch-Point Heating, Sustainability, 17 (2025) 19, 8664, DOI: 10.3390/su17198664

[4] Indrajith, B., Gunawardane, K.: Navigating the Intersection of Microgrids and Hydrogen: Evolutionary Trends, Challenges, and Future Strategies, Energies, 18 (2025) 3, p. 614, DOI: 10.3390/en18030614

[5] Böhm, M., Del Rey, A.F., Pagenkopf, J., Varela, M., Herwartz-Polster, S., Calderón, B. N.: Review and comparison of worldwide hydrogen activities in the rail sector with special focus on on-board storage and refueling technologies, International Journal of Hydrogen Energy, 47 (2022) 89, pp. 38003-38017, DOI: 10.1016/j.ijhydene.2022.08.279

[6] Mitrofanov, S.V., Kiryanova, N.G., Gorlova, A.M.: Stationary hybrid renewable energy systems for railway electrification: A review, Energies, 14 (2021), 5946, DOI: 10.3390/en14185946

[7] Le, T.S., Nguyen, T.N., Bui, D.K., Ngo, T.D.: Optimal sizing of renewable energy storage: A techno-economic analysis of hydrogen, battery and hybrid systems considering degradation and seasonal storage, Applied Energy, 336 (2023), 120817, DOI: 10.1016/j.apenergy.2023.120817

[8] Van, L.P., Do Chi, K., Duc, T.N.: Review of hydrogen technologies based microgrid: Energy management systems, challenges and future recommendations, International Journal of Hydrogen Energy, 48 (2023) 38, pp. 14127-14148, DOI: 10.1016/j.ijhydene.2022.12.345

[9] Marocco, P., Ferrero, D., Lanzini, A., Santarelli, M.: Optimal design of stand-alone solutions based on RES+ hydrogen storage feeding off-grid communities, Energy Conversion and Management, 238 (2021), p. 114147, DOI: 10.1016/j.enconman.2021.114147

[10] PV*Sol premium 2025 (Photovoltaic design and simulation), https://valentin-software.com/en/products/pvsol-premium/, 20.02.2026.

[11] Ng, W.K., Wong, W.Y., Rosli, N.A.H., Loh, K.S.: Commercial anion exchange membranes (AEMs) for fuel cell and water electrolyzer applications: performance, durability, and materials advancement, Separations, 10 (2023) 8, 424, DOI: 10.3390/separations10080424

[12] Meyer, Q., Ronaszegi, K., Pei-June, G., Curnick, O., Ashton, S., Reisch, T., Adcock, P., Shearing, P.R., Brett, D.J.: Optimisation of air cooled, open-cathode fuel cells: Current of lowest resistance and electro-thermal performance mapping, Journal of Power Sources, 291 (2015), pp. 261-269, DOI: 10.1016/j.jpowsour.2015.04.101

[13] Weniger, J., Orth, N., Meissner, L.: Energy Storage Inspection 2025, HTW Berlin, 2025.